Mechanisms of Air Cathode Pore Structure Parameters and Discharge Regimes on the Performance of Lithium–Air Batteries

Junlong Chen, Biyi Huang, Li Yang, Shan Gu, Zhenzhen Shi, Ru Yang, and Xianfeng Yu

Abstract As the society pays more attention to energy, various kinds of new energy batteries are coming out. Lithium–air battery is a new energy battery that uses lithium metal as the anode and oxygen in air as the positive reactant. Because of its specific energy comparable to that of fuel cells, lithium–air batteries are the most popular research in the direction of new energy batteries in the past few years. However, there are still some disadvantages of Li–air batteries that prevent them from being commercialized well, such as the accumulation of discharge products in the pores of the cathode, which leads to premature termination of the discharge reaction. Therefore, it is necessary to simulate the battery to investigate the existing problems. In this paper, we focus on the effects of lithium-air battery cathode porosity and discharge current density on battery performance and propose certain optimization strategies to address these problems.

Keywords New energy · Lithium–air batteries · Cathode porosity · Discharge current density
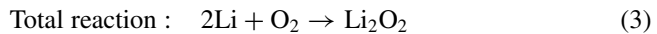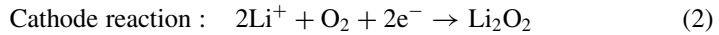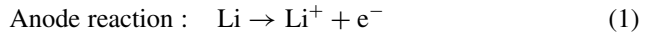
1 Introduction

With global warming and the global energy crisis, new energy electric vehicles are receiving more attention in the world. Lithium-air batteries (LABs) have been attracting attention for their high specific energy (11,400 Wh/kg) [1]. Depending on the electrolyte, LABs can be classified into organic system LABs, aqueous electrolyte LABs, organic-water hybrid electrolyte LABs, and all-solid electrolyte LABs, among which organic system LABs have been widely studied due to their simple structure and high energy density. The discharge reaction equation of organic LABs is shown in

J. Chen · B. Huang (✉) · L. Yang · S. Gu · Z. Shi · R. Yang · X. Yu
Zhejiang-Belarus Joint Laboratory of Intelligent Equipment and System for Water Conservancy and Hydropower Safety Monitoring, Zhejiang University of Water Resources and Electric Power, Hangzhou, China
e-mail: huangby@zjweu.edu.cn

Eqs. (1–3), whose anode is generally lithium monomer, which provides the lithium source required for the reaction, and the cathode is a porous material with good reactivity and large specific surface area. Having an open structure is one of the characteristics of LABs, where Li^+ reacts directly with oxygen from the air at the cathode. Li_2O_2 is formed and deposited on the cathode surface during discharge, while Li_2O_2 is oxidized and decomposed during charging [2].

$$\text{Anode reaction}: \quad Li \rightarrow Li^+ + e^- \tag{1}$$

$$\text{Cathode reaction}: \quad 2Li^+ + O_2 + 2e^- \rightarrow Li_2O_2 \tag{2}$$

$$\text{Total reaction}: \quad 2Li + O_2 \rightarrow Li_2O_2 \tag{3}$$

However, the specific capacity of LABs is often much lower than the theoretical value during the actual cycling process, which is due to the insoluble discharge product Li_2O_2 formed at the cathode during the discharge process. With Li_2O_2 continuously generated, the pores in the cathode are gradually blocked, and it is difficult for oxygen in the air to enter the cathode for reaction. In addition, Li_2O_2 has poor electrical conductivity and affects the electron transfer on the electrode surface, which reduces the battery capacity and cycling performance.

Therefore, designing a reasonable air transport path is of great importance to improve the cell performance of LABs [3]. Zhang et al. [4] used KB600 and Super P, materials with different porosity, to make composite electrodes, and the obtained electrodes exhibited higher air transfer capability by mixing KB600 with Super P in a 5:1 weight ratio. Tan et al. [5] prepared a gradient 100–500 μm gradient porous cathode for non-aqueous LABs with extremely high discharge capacity, thus demonstrating that the gradient porous distribution is necessary for the performance enhancement of LABs. In order to further explore the influence of each parameter of the battery on the battery performance, it is necessary to simulate and analyze the mechanism of the internal working process of the battery [6]. Sergeev et al. [7] developed a pore size distribution model for LABs and investigated the relationship between the pore size and the battery performance, concluding that the introduction of larger pore sizes has a significant enhancement of the battery capacity. Li et al. proposed a linear gradient pore structure and demonstrated that the use of linear porous air cathodes resulted in higher specific capacity, more uniform porosity, and more desirable oxygen diffusion coefficients for LABs. In addition, the discharge current density also affects the variation of electrode porosity, which changes the cell capacity [8]. Zhang et al. [9] found that the discharge capacity of LABs decreased sharply with increasing the discharge current density from 0.1 to 0.5 mA/cm^2 at the same electrode thickness. By studying the performance of the porosity LABs at discharge current densities of 0.05 and 0.5 mA/cm^2. Zhang et al. [10] concluded that if the range of the porosity gradient is too large at higher discharge current densities, it will lead to a significant increase in the overpotential of the battery, which will affect the performance of the battery. In summary, the porosity distribution of the

electrode has a very important effect on the performance of LABs, so it is necessary to investigate the effect of the initial porosity distribution and the discharge regime on the performance of LABs. Therefore, this paper constructs an electrochemical model of organic LABs with the help of Comsol software platform to systematically investigate the influence mechanisms of air cathode pore structure parameters and discharge regimes on the battery performance.

2 LABs Moddel

In this paper, a LAB with organic electrolyte is used as the research object, and its schematic diagram is shown in Fig. 1a. When the lithium-air works, the outer air of the cathode diffuses into the pore and reacts with the lithium ions in the electrolyte at the cathode to form lithium peroxide; the lithium monomer at the anode loses electrons to form lithium ions into the cathode. Assuming that the material transport process occurs only in the direction of the cell thickness, the cell can be simplified to a line, so the one-dimensional spatial dimension is chosen to construct the LAB model in this paper (Fig. 1b).

Inside the air cathode, oxygen diffusion, Li^+ diffusion and migration in the electrolyte, electron load transport in the porous carbon skeleton of the air cathode, and discharge product deposition and decomposition phenomena mainly occur. For the above complex physicochemical phenomena, the following assumptions are made:

- the convective transfer phenomena caused by the discharge product generation and decomposition are not considered;
- the initial solubility of oxygen in the electrolyte is saturated during the discharge process, and the solubility of oxygen in the electrolyte is constant;
- the products in the air cathode during the discharge process are all Li_2O_2;
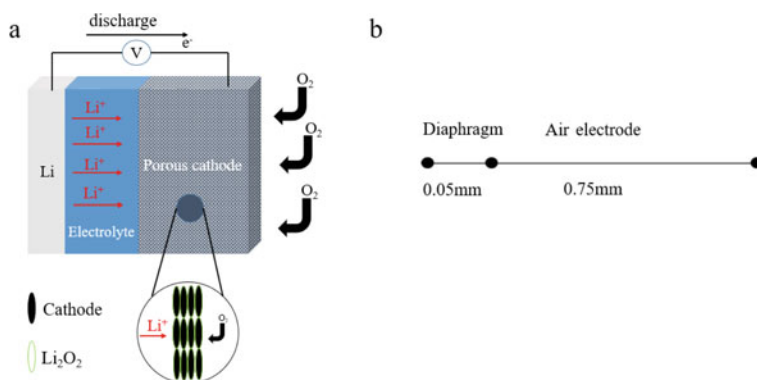

Fig. 1 Model of organic electrolyte LAB

- the electrochemical reactions of both positive and anodes satisfy the Butler-Volmer equation.

The internal control equations and boundary conditions of the non-aqueous LABs during discharge are listed below.

The potential of the cathode can be expressed by Eq. (4):

$$K_{pos}\nabla\phi_s - a_{pos}J = 0 \tag{4}$$

K_{pos} is the electrical conductivity and ϕ_s is the potential of the cathode, and the change of ϕ_s represents the change in the output voltage of the cell due to grounding the anode. a_{pos} signifies the specific surface area of the air cathode diaphragm, whose expression is given in Eq. (5). J manifests the current density of the cathode, which can generally be described by the Buster-Volmer equilibrium method, whose expression is given in Eq. (6).

$$a_{pos} = a_{pos}\left[1 - \frac{\varepsilon_{Li_2O_2}}{\varepsilon_{l0}}\right] \tag{5}$$

$$J = nF\left[K_c(c_{Li})^2 C_{O_2}\exp\left(\frac{0.5nF\eta}{RT}\right) - K_a C_{Li_2O_2}\exp\left(\frac{-0.5nF\eta}{RT}\right)\right] \tag{6}$$

a_{pos0} is the initial active specific surface area of the anode, and the relevant parameters are shown in Table 1. $\varepsilon_{Li_2O_2}$ is the volume fraction of Li_2O_2, and its expression is given in (7), and ε_{l0} indicates the initial porosity. n is the number of electrons transferred, $F = 96{,}487$ C/mol, which represents the Faraday constant. η means the overpotential, whose expression is given in (8), K_a represent the reaction rate coefficient of the metal Li, and K_c is the reaction rate coefficient of the cathode. R implies the molar gas constant, which is ~ 8.314472, T represents the temperature.

$$\varepsilon_{Li_2O_2} = \left(c_{Li_2O_2} - c_{0,Li_2O_2}\right) \times \frac{M_{Li_2O_2}}{\rho_{Li_2O_2}} \tag{7}$$

$$\eta = \phi_s - \phi_l - \Delta\phi_{flim} - E_{eq} \tag{8}$$

$c_{Li_2O_2}$ denotes the concentration of Li_2O_2 at any moment, c_{0,Li_2O_2} means the initial Li_2O_2 concentration, $M_{Li_2O_2}$ and $\rho_{Li_2O_2}$ signifies respectively the molecular weight of Li_2O_2 and the density of Li_2O_2, ϕ_l represents the electrolyte potential, E_{eq} is the equilibrium voltage. $\Delta\phi_{flim}$ denotes the membrane resistance voltage, the expression of which is given in (9). R_{flim} represents the membrane resistance of the membrane in Eq. (9).

$$\Delta\phi_{flim} = JR_{flim}\varepsilon_{Li_2O_2} \tag{9}$$

Table 1 Model initial values and related parameters

Parameters	Symbol	Value	Parameters	Symbol	Value
The length of the diaphragm [8]	L_{sep}	5×10^{-5} m	Diffusion coefficient of Li$^+$ in electrolyte [8]	D_{Li}	2.11×10^{-9} m^2/s
Length of air cathode	L_{pos}	7.5×10^{-4} m	Oxygen diffusion coefficient [8]	D_{O_2}	7×10^{-10} m^2/s
Conductivity of cathode [11]	K_{pos}	10 S/m	Conductivity of Li$^+$ in electrolyte [8]	K_{Li}	1.085 S/m
Initial porosity of air cathode [8]	ε_{l0}	0.73	Transference number of Li$^+$ in electrolyte [8]	t^+	0.2594
Initial active material solid fraction of cathode	ε_{s0}	0.27	Reaction rate coefficient anodic current [8]	K_a	1.11×10^{-15} m/s
Porosity of separator [8]	ε_{sep}	0.87	Reaction rate coefficient cathodic current	K_c	3.4×10^{-17} m^7/s/mol^2
Particle radius in the cathode [8]	r_{pos0}	25×10^{-9} m	Reference exchange current density Li metal	i_{0refLi}	9.65×10^{-1} A/m^2
Initial active specific surface area in cathode	a_{pos0}	3.24×10^7 m^{-1}	Equilibrium potential for oxygen reduction reaction [8]	E_{eq}	2.96 V
Film resistance across Li$_2$O$_2$ film [8]	R_{film}	50 Ω*m^2	Number of transferred electrons [8]	N	2
Reference concentration of Li$^+$ [8]	c_{Li0}	1000 mol/m^3	Density of Li$_2$O$_2$ [8]	$\rho_{Li_2O_2}$	2140 kg/m^3
Solubility factor of oxygen in electrolyte [8]	Sol_{O_2}	0.4	Molecular weight of Li$_2$O$_2$ [7]	$M_{Li_2O_2}$	45.88×10^{-3} kg/mol
External oxygen concentration in air at 1 atm [8]	c_{O_2ext}	9.46 mol/m^3	Density of carbon [7]	ρ_{carbon}	2260 kg/m^3
Initial oxygen concentration in cathode	c_{O_20}	3.784 mol/m^3	Temperature [8]	T	300 K
Solubility limit of Li$_2$O$_2$ dissolved in electrolyte [8]	$c_{maxLi_2O_2}$	0.09 mol/m^3	Applied current density	i_{-app}	$-0.05 \times a$ mA/cm^2

The current density J_1 of another lithium metal as the anode can be obtained from the Buster-Volmer equilibrium method, the expression of which is given in (10), where i_{0refLi} is the negative exchange current density.

$$J_1 = i_{0refLi}\left(\exp\left(\frac{0.5nF\eta}{RT}\right) - \exp\left(\frac{-0.5nF\eta}{RT}\right)\right) \tag{10}$$

As mentioned previously, the effective diffusion coefficients of oxygen and lithium ions are shown in Eqs. (11) and (12) when convection is not considered in the whole model and the Bruggeman model is chosen for the effective diffusion coefficient model.

$$D_{e,O_2} = \varepsilon^{1.5} D_{O_2} \tag{11}$$

$$D_{e,Li^+} = \varepsilon^{1.5} D_{Li} \tag{12}$$

As the discharge of the LABs proceeds, Li_2O_2 precipitation is produced, and the domain ordinary differential and differential algebraic equations are applied in Comsol to analyze whether Li_2O_2 precipitation occurs in the cell. The relevant expressions are given in (13).

$$d_a \frac{\partial c_{Li_2O_2}}{\partial t} = \frac{1}{2F} i_{vtot}\left(c_{Li_2O_2} > c_{\max\ Li_2O_2}\right), \tag{13}$$

d_a is the damping or quality factor, taken as 1. i_{vtot} is the electrode reaction source. Equation (13) shows that precipitation occurs when the concentration of Li_2O_2 in the electrolyte exceeds the dissolution limit of dissolved Li_2O_2 in the electrolyte.

The pore utilization rate shows in Eq. (14). S is pore utilization rate, S_0 indicates the integrated area of initial porosity and S_t indicates the integrated area of porosity after a certain time of discharge.

$$S = \frac{(S_0 - S_t)}{S_0} \times 100\% \tag{14}$$

Finally, the system is set up with the cell size of the grid partition for the finer refinement. The initial porosity of the cathode of the cell is 0.73, and the condition of reaction stop in the cell is set at 2.5 V. The initial values of other parameters are detailed in Table 1.

3 Results and Discussion

To investigate the effect of different porosities on the performance of LABs, three pore structures were selected for comparison. Single porosity, i.e., the cathode has a unique porosity $\varepsilon = 0.73$; linearly varying porosity, i.e., the cathode porosity changes linearly with the electrode thickness direction, from the inner side of the cell to the outer side of the air as $\varepsilon = 0.63 \sim 0.83$; gradient porosity, i.e., the cathode porosity is divided into two kinds along the thickness direction, with the inner half as $\varepsilon = 0.63$ and the outer half as $\varepsilon = 0.83$, which is expressed in the text as $\varepsilon = 0.63–0.83$. The oxygen concentrations along the electrode thickness direction for different porosities are given in Fig. 2. All electrodes exhibit higher oxygen concentration on the air side, which gradually decreases with the electrode thickness direction, indicating that there is a resistance to oxygen diffusion into the interior of the electrode. From Fig. 2a, it can be seen that the electrode with gradient porosity has the highest internal oxygen concentration, followed by the linear porosity electrode, and the single porosity electrode has the lowest oxygen concentration, indicating that the gradient porosity is conducive to the diffusion of oxygen to the internal. When the discharge current density increased to 0.5 mA/cm^2 (Fig. 2b), the oxygen concentration on the outer side of the electrode decreased sharply, and very little oxygen could diffuse into the inner part of the electrode to participate in the reaction.
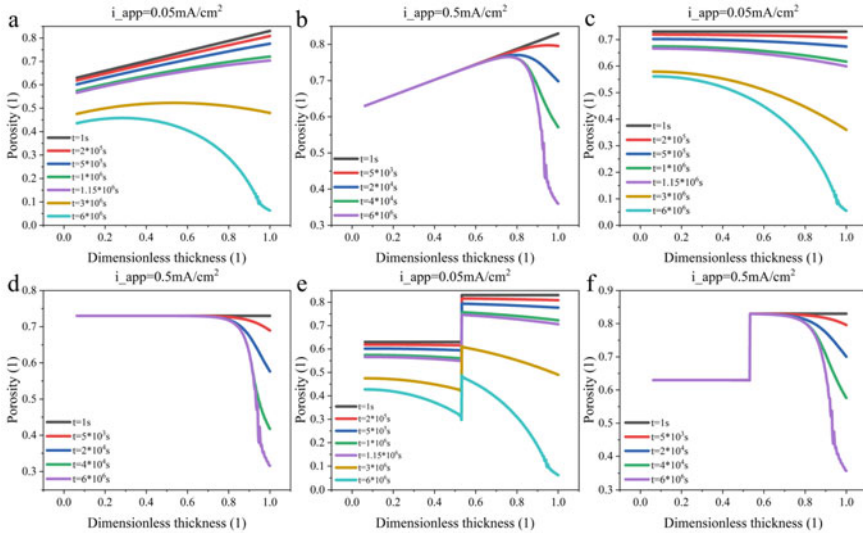
The variation of porosity at different current densities is given in Fig. 3. The pore utilization rate was calculated by Eq. (14) and is shown in Table 2. The difference between the utilization rate of linear porosity and single porosity in the early stage is not significant, which is due to the short time of discharge, and as the discharge time continues, the utilization rate of linear porosity is greater than that of single porosity. At the discharge current density of 0.05 mA/cm^2, the utilization rate of the
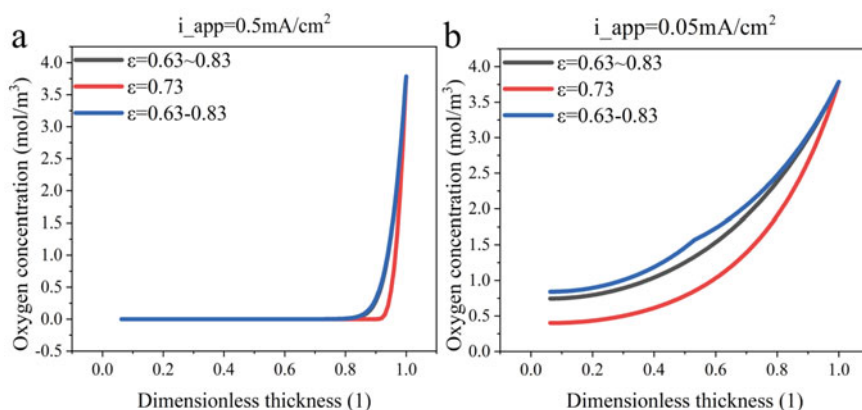
Fig. 2 Oxygen concentration of cathode with different porosities. **a** Discharge time $= 3*10^6$ s; **b** Discharge time $= 4*10^4$ s

cathode with the gradient porosity structure increased substantially and more Li_2O_2 was precipitated inside the air cathode with time.

When the discharge current density increases to 0.5 mA/cm², a large amount of Li_2O_2 collects on the air side of the electrode, which causes a significant decrease in the utilization rate inside the air cathode. In contrast, the gradient porosity structure has a higher electrode pore utilization, indicating that it is more favorable for the


Fig. 3 Porosity variation at different discharge current densities. **a**, **b**: $\varepsilon = 0.63 \sim 0.83$; **c**, **d** $\varepsilon = 0.73$; **e**, **f** $\varepsilon = 0.63–0.83$

Table 2 Electrode pore utilization at different pore gradients

Porosity	0.73	0.63 ~ 0.83	0.63–0.83
Utilization at 0.05 mA/cm² ($t = 1$ s)	0%	0%	0%
Utilization at 0.05 mA/cm² ($t = 2*10^5$ s)	2.0%	2.0%	4.6%
Utilization at 0.05 mA/cm² ($t = 5*10^5$ s)	5.1%	5.1%	7.6%
Utilization at 0.05 mA/cm² ($t = 1*10^6$ s)	10.1%	10.1%	12.5%
Utilization at 0.05 mA/cm² ($t = 1.15*10^6$ s)	11.6%	11.6%	14.0%
Utilization at 0.05 mA/cm² ($t = 3*10^6$ s)	30.4%	30.4%	32.3%
Utilization at 0.05 mA/cm² ($t = 6*10^6$ s)	42.1%	49.4%	53.1%
Utilization at 0.5 mA/cm² ($t = 1$ s)	0%	0%	0%
Utilization at 0.5 mA/cm² ($t = 5*10^3$ s)	0.4%	0.4%	3.1%
Utilization at 0.5 mA/cm² ($t = 2*10^4$ s)	2.0%	2.0%	4.6%
Utilization at 0.5 mA/cm² ($t = 4*10^4$ s)	4%	4%	6.6%
Utilization at 0.5 mA/cm² ($t = 6*10^6$ s)	5%	6.7%	9.3%
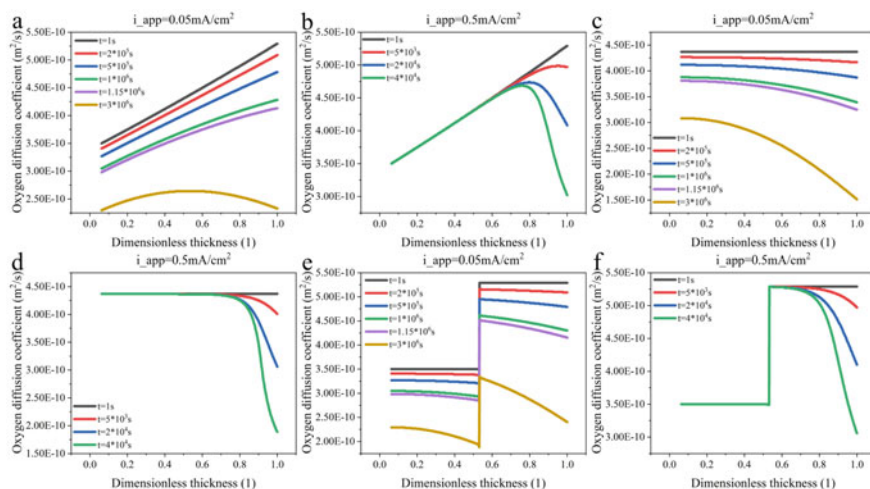
Fig. 4 Effective oxygen diffusion coefficient with different porosities. **a, b** ε = 0.63 ~ 0.83; **c, d** ε = 0.73; **e, f** ε = 0.63–0.83

storage of discharge products at high current densities. Overall, compared with single porosity, gradient or linear porosity can provide more Li_2O_2 storage space on the air side and prevent pores from being blocked prematurely during the discharge process.

Oxygen is an important reactant in the discharge process, and its content and diffusion rate inside the electrode affect the generation of discharge products. The effective diffusion coefficients of oxygen at different porosities are given in Fig. 4. From the figure, it can be obtained that the oxygen diffusion coefficient inside the electrode decreases continuously as the discharge proceeds, and it decreases to a greater extent on the outside of the electrode. Because the outer side possesses more oxygen, Li_2O_2 is more likely to accumulate on the outer side of the electrode, causing the area to be blocked (as shown in Fig. 3).

At a current density of 0.05 mA/cm^2, the oxygen diffusion coefficient inside the electrode decreases gradually with a single porosity, and the decrease is greater at the oxygen inlet. Li_2O_2 accumulates first in the oxygen-rich part of the electrode, so the electrode is more likely to be blocked at the oxygen inlet, resulting in limited oxygen conduction. The above problem can be greatly improved by the linear porosity or gradient porosity electrodes, where the porosity at the oxygen inlet side is larger than at the electrode interior. As can be seen from the figure, the oxygen diffusion coefficients outside the electrodes of two composite porosities are still larger than those inside the electrodes with the reaction at lower discharge current densities, which is favorable to the oxygen transport inside the electrodes. When the discharge current density is 0.5 mA/cm^2, the oxygen diffusion coefficient of each electrode decreases rapidly at the oxygen inlet side, and the decrease is most serious for the electrode with single porosity.

Figure 5 gives the battery discharge curves under different porosities, and it can be seen the gradient porosity cathode has the largest cell specific capacity. From the previous analysis, it can be seen that the air cathode with gradient porosity has a larger pore structure on the air side, which can store more Li_2O_2 during the discharge process without causing pore blockage, which is conducive to the continuous diffusion of oxygen to the interior of the electrode, increasing the oxygen content inside the electrode and promoting the electrochemical reaction inside the cell. As more substances are involved in the cell reaction, the battery capacity is improved accordingly. The specific capacity and discharge voltage of the cell for each porosity are significantly reduced when the discharge current density is increased to 0.5 mA/cm^2. The high current density leads to the accelerated rate of Li_2O_2 production, the rapid deposition of Li_2O_2 on the air side to block the pores of the electrode, and the low utilization of the active material inside the electrode, which manifests as the decrease of the battery capacity. The decrease in discharge voltage is due to the polarization of the electrode caused by the excessive discharge current density.

However, among the general air cathodes, the porosity of the cathode has a certain randomness along the electrode thickness direction, so it is necessary to explore the effect of random porosity on the battery performance. A new random function rn1 can be added to the definition in Comsol, and the average porosity of the raw composition is at 0.73, and the random porosity distribution of the electrode with a range of 0.2 is shown in Fig. 6a. Figure 6b compares the discharge performance of the two porosity electrodes, the scatter plot indicates the voltage of the cell under single porosity, and the line graph indicates the voltage of the cell under random porosity, and it can be obtained that the specific capacity of the cell in the case of random porosity is slightly larger than that of single porosity.

As can be seen from Fig. 6a, the porosity of the air side of the air cathode with random porosity is higher than the average pore size of 0.73, which provides storage space for insoluble discharge products while also providing a transport channel for oxygen. Therefore, the film thickness of insoluble discharge products in the air cathode with random porosity is no longer smooth along the electrode thickness
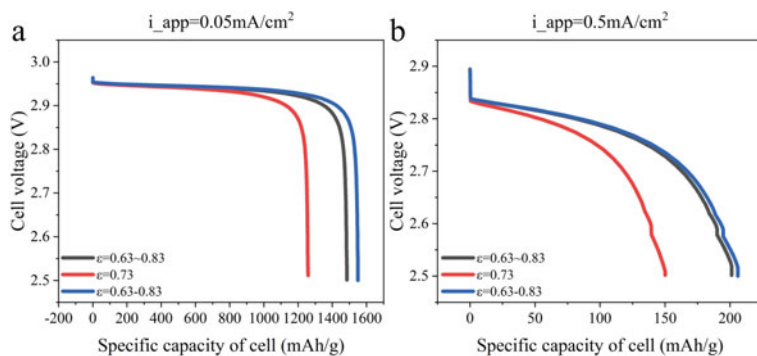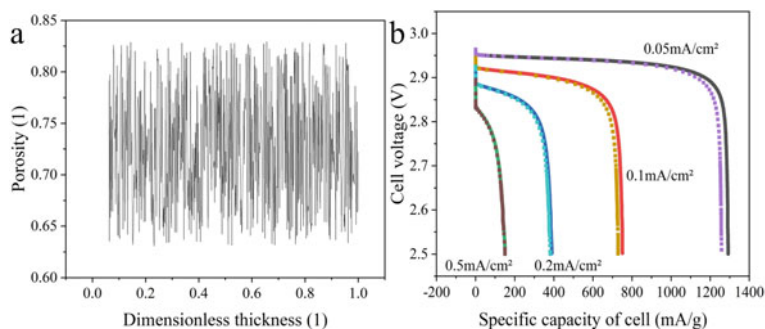

Fig. 5 Cell voltage at different porosities

Fig. 6 Random porosity distribution and cell voltage comparison

direction, and the probability of total blockage at the same discharge moment is relatively small compared with that of the air cathode with constant porosity.

4 Conclusion

- The porosity of the cathode largely affects the battery performance, and the use of linear porosity in the cathode provides better performance compared to gradient porosity and single porosity. The role of linear porosity is reflected in various characteristics of LABs, such as optimization of porosity distribution, oxygen concentration, effective oxygen diffusion coefficient, etc. during the discharge process. The adoption of linear porosity in the anode prevents the external pores from being blocked prematurely during discharge, oxygen is fully supplied and diffused inside the electrode, and the utilization rate inside the electrode is improved, which greatly improves the battery performance.
- LABs reaction occurs mainly on one side of the air cathode boundary, and the outer side of the cathode has more oxygen, so Li_2O_2 is more likely to accumulate on the outer side of the electrode. It can be concluded that for battery operation, the larger porosity of should be near the air side to allow more storage space for discharge products.
- In actual preparation, the porosity of the cathode has a certain randomness along the electrode thickness direction. If at random porosity and its average porosity is the same as that of the evidence electrode with a single porosity, the cell has a higher specific capacity compared to that of the cathode with a single porosity.

References

1. Albertus P et al (2011) Identifying capacity limitations in the Li/oxygen battery using experiments and modeling. J Electrochem Soc 158:A343
2. Peng Z, Freunberger SA, Chen Y, Bruce PG (2012) A reversible and higher-rate Li-O$_2$ battery. Science 337:563–566
3. Meng J et al (2017) Advances in structure and property optimizations of battery electrode materials. Joule 1:522–547
4. Zhang Y et al (2013) The use of mixed carbon materials with improved oxygen transport in a lithium-air battery. J Power Sour 240:390–396
5. Tan P, Shyy W, An L, Wei Z, Zhao T (2014) A gradient porous cathode for non-aqueous lithium-air batteries leading to a high capacity. Electrochem Commun 46:111–114
6. Elabyouki M, Bahamon D, Khaleel M, Vega LF (2019) Insights into the transport properties of electrolyte solutions in a hierarchical carbon electrode by molecular dynamics simulations. J Phys Chem C 123:27273–27285
7. Sergeev AV, Chertovich AV, Itkis DM (2016) Modeling of the lithium-air battery cathodes with broad pore size distribution. Chem Phys Lett 660:149–154
8. Li J et al (2020) Highly efficient Li–air battery using linear porosity air electrodes. J Electrochem Soc 167:090529
9. Zhang G et al (2010) Lithium–air batteries using SWNT/CNF buckypapers as air electrodes. J Electrochem Soc 157:A953
10. Zhang T et al (2022) Effect of porosity gradient on mass transfer and discharge of hybrid electrolyte lithium-air batteries. J Energy Stor 46:103808
11. Sahapatsombut U, Cheng H, Scott K (2013) Modelling the micro–macro homogeneous cycling behaviour of a lithium–air battery. J Power Sour 227:243–253